

TTF3 POWER COUPLER THERMAL ANALYSIS FOR LCLS-II CW OPERATION*

L. Xiao, C. Adolphsen, Z. Li, C. Nantista and T. Raubenheimer, SLAC, Menlo Park, CA, USA,
N. Solyak and I. Gonin, FNAL, Batavia, IL, USA

Abstract

The TESLA 9-cell SRF cavity design has been adopted for use in the LCLS-II SRF Linac. Its TTF3 coaxial fundamental power coupler (FPC), optimized for pulsed operation in European XFEL and ILC, requires modest changes to make it suitable for LCLS-II continuous-wave (CW) operation. For LCLS-II it must handle up to 7 kW of power, fully reflected, with the maximum temperature around 450 K, the coupler bake temperature. In order to improve TTF3 FPC cooling, an increased copper plating thickness will be used on the inner conductor of the 'warm' section of the coupler. Also the antenna will be shortened to achieve higher cavity Qext values. Fully 3D FPC thermal analysis has been performed using the SLAC-developed parallel finite element code suite ACE3P, which includes electromagnetic codes and an integrated electromagnetic, thermal and mechanical multi-physics code. In this paper, we present TTF3 FPC thermal analysis simulation results obtained using ACE3P as well as a comparison with measurement results.

INTRODUCTION

The TTF3 FPC, depicted in Fig. 1, brings 1.3 GHz RF power from an external waveguide feed to an SRF cavity inside a cryomodule via a coaxial structure incorporating two cylindrical vacuum windows and bellows for Qext tuning. The design was developed for pulsed operation, as in XFEL and ILC.

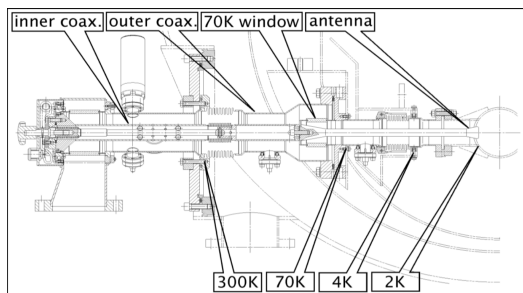


Figure 1: TTF3 FPC design. The FPC is made of copper plated stainless steel except for the cold-part center conductor antenna, which is made of solid copper (courtesy of DESY).

Past studies suggest its suitability up to at most 5 kW in standing-wave CW operation [1], less than the 7 kW required (worst case) for LCLS-II. The plating on the stainless steel inner conductor of the warm section will be

increased from 30 μm to 150 μm to significantly lower its peak temperature to a level comparable to that during its bake-out (450 K). In addition, the antenna tip will be trimmed by 8.5 mm to increase the mid-range Qext value. For the low-current LCLS-II beams, Qext will be set to 4×10^7 , about 10 times higher than for ILC.

Fully 3D LCLS-II FPC thermal analysis was performed using the SLAC developed ACE3P, a comprehensive set of conformal, higher-order, parallel finite-element electromagnetic codes with multi-physics capabilities in integrated electromagnetic, thermal and mechanical simulation [2]. TEM3P is ACE3P's multi-physics module. Its thermal capabilities include non-linear thermal conductivity in near superconducting condition, non-linear heat flux and convective boundary conditions for fluid-solid interface, shell elements for surface coating and volume RF heating for ceramic window loss.

2D SIMULATION BENCHMARKING

TTF3 FPC thermal simulations have been carried out using commercial software, such as ANSYS and COMSOL [3][4]. Because of single processor memory limitation, the FPC thermal simulations have been limited to its 2D model. In order to benchmark with COMSOL, a one-sixteenth slice of the FPC 2D structure, as shown in Fig. 2, was simulated using TEM3P. The second order tetrahedral meshes having 100k and 660k mesh elements for RF and thermal modelling, respectively are shown in Fig. 3.

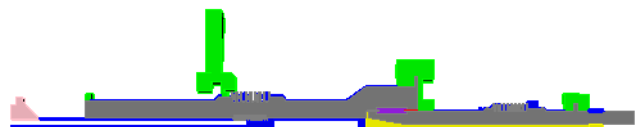


Figure 2: A wedge model of the LCLS-II FPC.

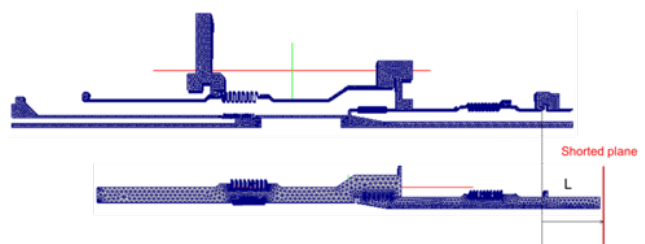


Figure 3: LCLS-II FPC meshes for thermal (upper) and RF (lower) simulations.

A shorting plane at varied locations was used to simulate cavity reflection for various frequency detunings. For this study, a 10 μm and 100 μm copper layer was assumed on the outer and inner stainless steel

* Work supported by the Department of Energy under Contract Number: DE-AC02-76SF00515.

conductors, respectively. Shell elements were implemented to represent the plating without actually introducing the thin layers in the simulation model. Use of shell elements controls the total number of mesh elements and thus saves computational resources.

The EM fields were first calculated in the FPC vacuum and ceramic region using ACE3P-S3P, an S-parameter solver. Then the power losses on the surfaces as well as in the window were used as the heat load input for the thermal simulation using ACE3P-TEM3P. The thermal and RF models share the same common surface meshes at their interfaces, so that the heat flux can be transferred directly between the two analyses. The thermal analysis was done for the metal region with the temperature assumed fixed on three surfaces (with is achieved in the cryomodule by thermal anchoring).

The maximum temperature on the LCLS-II FPC vs. shorting position is plotted in Fig. 4 for 7 kW input power. The material thermal properties used in the simulations are shown in Figure 5. The TEM3P results agree very well with those obtained with COMSOL by FNAL[4]. One simulation from TEM3P uses 256 processors on NERSC's Hopper machine and can be completed within 30 mins.

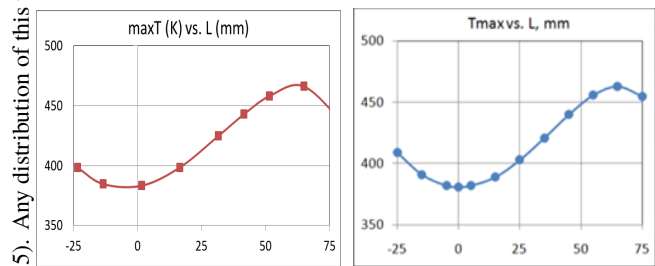


Figure 4: Maximum temperature vs. short location calculated by TEM3P (left) and COMSOL (right).

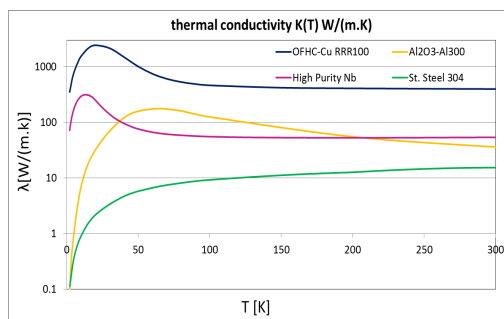


Figure 5: FPC material thermal conductivities.

3D SIMULATION

Parallel implementation of ACE3P makes fully 3D LCLS-II FPC thermal analysis possible. The thermal and RF meshes used for 3D simulations are shown in Fig. 6.

In general, the maximum temperature in the 3D simulation was higher than in 2D, as shown in Fig. 7. With the cavity on-resonance and $Q_L=4 \times 10^7$, corresponding to the short at $L=33\text{mm}$ in Fig. 7, the maximum temperature is 476 K. The maximum temperature is on

the warm inner conductor, close to the bellows. The temperature and magnetic field map for on-resonance operation are shown in Fig. 8.

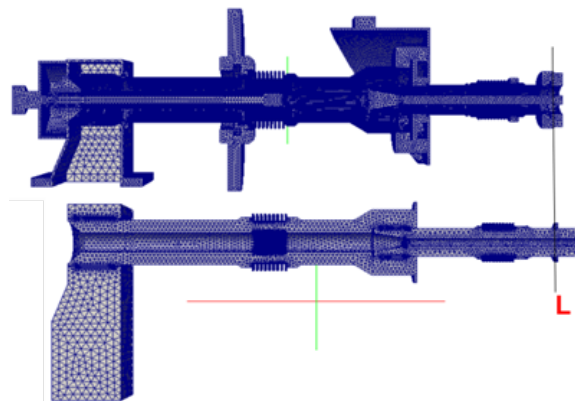


Figure 6: 3D LCLS-II FPC meshes for thermal (top) and RF simulations (bottom).

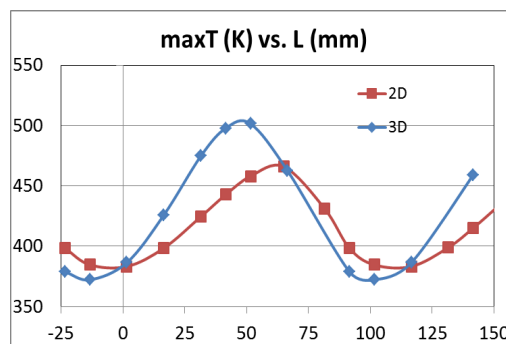


Figure 7: The maximum temperature vs. short location computed in 2D and 3D simulations.

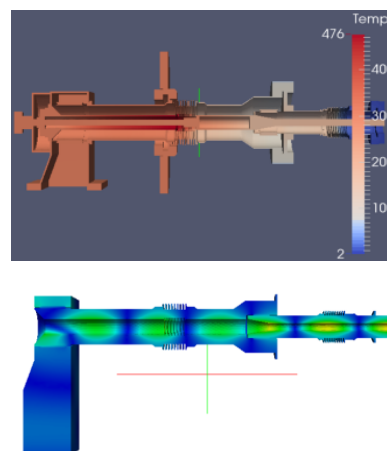


Figure 8: Temperature (upper) and magnetic field (lower) maps.

The calculated power losses in the LCLS-II FPC are listed in Table 1. It was found that the power losses on the waveguide walls and warm (outer) window contribute a large portion to the total and thus cause the maximum temperature rise to be higher in 3D simulation than in 2D. Therefore, fully 3D FPC thermal simulation is necessary.

Table 1: Power Loss Distribution in the LCLS-II FPC

Maximum Input Power 14 kW in TW										
Inner Conductor in Warm Section P (W)	Antenna P (W)	Cu WG P (W)	Ceramic Window P (W)	Outer Conductor in Cold Section P (W)	Outer Conductor in Warm Section P (W)					
Left Tube	8.4	11.7 (without tip)	4.9	$\epsilon_r=9$, $\tan \delta=3e-4$	Left Tube	1.7	Left Tube	5.7		
Bellow	5.4				Cold	5.4	Bellow	2.4	Bellow	2.5
Right Tube	4.1				Warm	14.8	Right Tube	1.1	Right Tube	3.1

HTS TESTS

The first LCLS-II FPC HTS (horizontal test stand) test was performed at FNAL with 6 kW input power [5]. Overheating of the “70 K” flange was observed due to inadequate thermal anchoring, and it reached over 300 K. The predicted (2D) temperature along the inner conductor computed by FNAL is plotted in Fig. 9 for both the ideal and actual temperatures at the thermal anchor locations. An infrared thermal sensor was used to measure the inner conductor temperature at one location, indicated by the vertical red line in Fig. 9. The 3D expectation for this temperature (purple star) agrees well with the measurement (red circle).

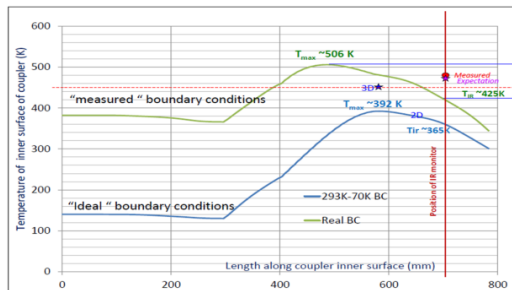


Figure 9: Temperature along the inner conductor at ideal and measured thermal boundary conditions (courtesy of FNAL).

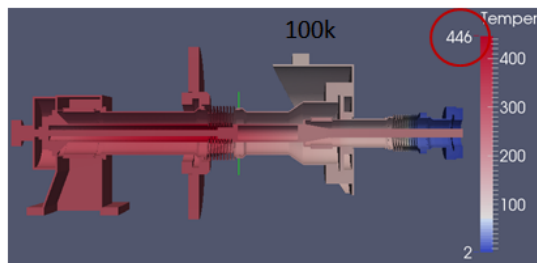


Figure 10: The temperature map in the worst scenario assuming the copper plating thickness of 150 μm on the inner conductor, 7 kW input power with full reflection and “70” K flange at 100 K.

After the first LCLS-II FPC HTS test, changes were implemented to improve the thermal connection, such as installing four new metal braids to replace the two old ones. A 3D FPC thermal simulation shows that if the “70 K” flange can be kept below 100 K and the copper plating on the inner conductor is 150 μm , the maximum

temperature will not exceed the 450 K, as shown in Figure 10.

HEAT LOADS

The LCLS-II cryogenic plant will provide cooling for the SC linac operation, and its sizing depends on the heat loads and other factors. Our simulations provide input in this regard. For example, Table 2 lists the RF related heat loads for a worse-case on-resonance scenario where 6.4 kW is input and 1.6 kW is reflected.

Table 2: Dynamic Heat Loads in LCLS-II FPC

Coupler Dynamic Heat Loads		
Coating thickness (μm) on the inner conductor	100	150
2 k Load (W)	0.12	0.12
4 k Load (W)	0.92	0.93
70 k Load (W)	15.99	16.73

ACKNOWLEDGMENTS

This work used the resources of NERSC at LBNL which is supported by the Office of Science of the US Department of Energy.

REFERENCES

- [1] J. Knobloch, *et al.*, “CW Operation of the TTF-III Input Coupler”, Proc. of PAC2005, Knoxville, TN, US
- [2] V. Akcelik, *et al.*, “Thermal Analysis of SRF Cavity Couplers Using Parallel Multiphysics Tool TEM3P”, Proc. of PAC2009, Vancouver, Canada
- [3] S. Pei, *et al.*, “RF Thermal and New Cold Part Design Studies on TTF-III Input Coupler for Project-X” <http://arxiv.org/ftp/arxiv/papers/1108/1108.2587.pdf>
- [4] N. Solyak, *et al.*, “LCLS-II Power Coupler”, AWLC2014, May 12-16, 2014, FNAL. <https://agenda.linearcollider.org/event/6301/session/10/contribution/275/material/slides/>
- [5] A. Hocker, “LCLS-II Coupler Test Results”, <https://slacspace.slac.stanford.edu/sites/lcls/lcls-2/ap/Pages/scrfl.aspx>